Korean J. Chem. Eng., **16**(5), 635-639 (1999)

Effect of Satellite Bubbles on Dynamics of Gas Absorption from a CO_2 Bubble into a Downward-Flowing Liquid

Katsumi Tsuchiya†, Masanobu Koshihata, Tahei Tomida and Takayuki Saito*

Department of Chemical Science and Technology, The University of Tokushima, Tokushima 770-8506, Japan
*Geotechnology Department, National Institute for Resources and Environment, Tsukuba 305-8569, Japan
(*Received 2 April 1999 • accepted 24 May 1999*)

Abstract–The dynamic process of gas absorption from a CO_2 bubble into a liquid is examined in the presence of satellite bubbles. The bubble under consideration is held stationary, except its jittering, by the liquid flowing downward. The mass transfer rate is determined by monitoring the rate of reduction in the equivalent bubble diameter during the initial absorption process. It is found that the interaction with the satellite bubbles generally hampers the dissolution of the primary bubble. The extent of reduction in the dissolution rate increases with the net contacting time during the interaction. When the secondary bubbles interact with the primary bubble mainly outside of its wake, however, the dissolution tends to be enhanced due to induced turbulence in the surrounding liquid flow. A simple theoretical model is developed to simulate the observed results as well as the basic features prevailing in a recently proposed scheme, called the GLAD system, for shallow injection of CO_2 gas into seawater.

Key words : Global Warming, Carbon Dioxide, Gas Absorption, Bubble Deformation, Turbulence Intensity

INTRODUCTION

Carbon dioxide needs to be reduced in its atmospheric concentration due to its ever-increasing role in global warming. As one promising *short-term* measure, a system called Gas Lift Advanced Dissolution (GLAD) has been recently proposed [Saito and Kajishima, 1997]. The GLAD system is primarily adapted for the treatment of exhaust gases from the firepower station near the seashore and, as shown in Fig. 1, uses an inverted J-shaped column submerged in the ocean. Compressed CO_2 gas is sparged into the shorter leg, or the riser, and leaves from the bottom of the longer leg, or the downcomer, as dissolved components in seawater. The upward motion of the liquid induces "suction" of fresh seawater at the riser bottom; CO_2-enriched seawater released from the downcomer bottom could by itself descend before significant dilution takes place to a deeper location.

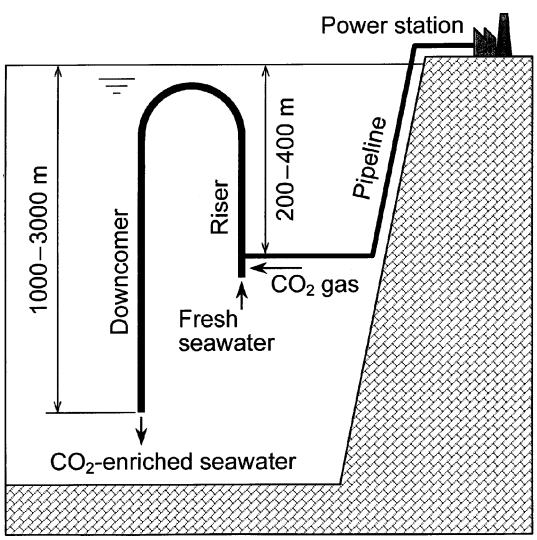

Fig. 1. Conceptual configuration of the GLAD system.

For bubbles containing a large fraction of a gaseous component of relatively high solubility such as CO_2, dissolution of the gas into a liquid proceeds with appreciable shrinkage in the bubble size. The dissolution process becomes further complicated if the interaction between neighboring bubbles is significant. In environmental applications which involve gas-dispersed multiphase flow, as in the GLAD riser, these complexities are often superimposed; the proper design and operation of the flow system require simultaneous analyses of local mass transfer and hydrodynamic characteristics of bubbles and the surrounding flow. Despite extensive research efforts over the last four decades toward a comprehensive description of the phenomena, information available in the literature is mostly fragmental [e.g., Calderbank and Moo-Young, 1961; Clift et al., 1978; Kawase et al., 1992].

In this study, the dynamic process of gas dissolution from a single CO_2-containing bubble into a liquid is examined in the absence/presence of secondary satellite bubbles. Both experimental and theoretical analyses are conducted. In the experiment, the primary bubble is held almost stationary by forcing the liquid to flow downward. The bubble behavior is monitored via a Charge-Coupled Device (CCD) camera and analyzed using an image processing system. The theoretical analysis lays its basis on modeling the dissolution process of a bubble comprising two components of different solubility. Formulated in a set of differential equations with general expressions for the perti-

†To whom correspondence should be addressed.
E-mail : kats@chem.tokushima-u.ac.jp

nent physical parameters, the model can be used to simulate the dissolution process under various conditions.

EXPERIMENTAL

The dynamic behavior of a CO_2 bubble is recorded via a digital CCD camera (Panasonic NV-DS5), and later analyzed frame by frame to estimate its size (volume-equivalent diameter) from the projected bubble area. If the gas phase within the bubble is assumed to be, at least initially, pure CO_2, the absorption rate of CO_2 into the liquid can be determined from the time variation of the bubble size. For detailed observation of the gas-liquid interface and the surrounding flow, a high-sensitivity CCD camera (Hamamatsu Photonics SuperEye® C2847) is utilized in its differential mode. Significantly enhanced in contrast through this camera, particles (~10-μm nylon beads) seeded in the liquid phase permit the movement of liquid elements in the vicinity of the bubble as well as the fluctuating bubble-surface boundary to be traced effectively.

The main apparatus used in this study, shown in Fig. 2, is the downward-liquid-flow column which consists of the tapered test section, topped with the liquid-flow straightening section, and the bubble injecting section below. The lateral distribution of downward liquid velocity in the test section is improved (more flattened) by the internal flow spoiler in the straightening section. Details of each section are described elsewhere [Tsuchiya et al., 1997]. Single bubbles of a fixed volume can be introduced by utilizing alternate on-off switching of Ball valves B and C. The initial bubble size is controlled by changing the volume of the compartment between these valves as well as by varying the gas supply pressure to the bubble injection line. Tap water or its NaCl solution is used as the liquid phase. The system of circulating liquid is pressurized by nitrogen at a desired level up to 0.6 MPa. The effect of salts content is examined over the NaCl concentration range 0–3 wt%, which corresponds to typical NaCl concentrations of seawater (up to 3.5 wt% in terms of total salts).

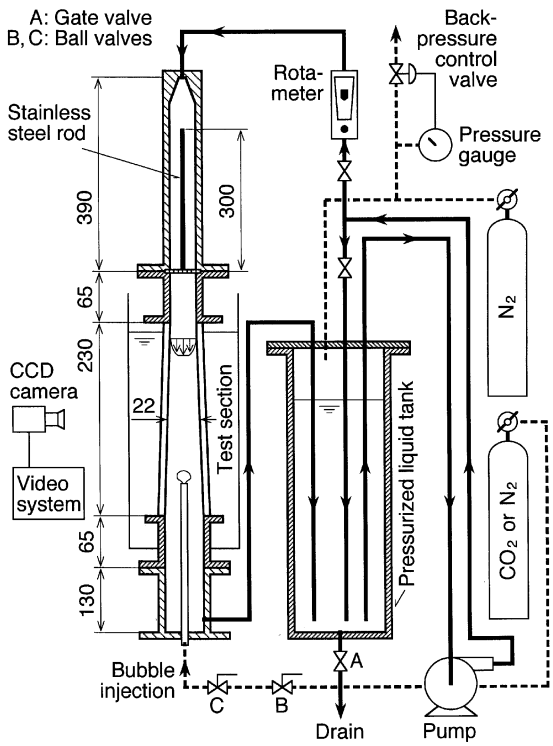

Fig. 2. Schematic diagram of the experimental apparatus.

MODELING

One of the important requirements in the GLAD technology is to achieve sufficient dissolution of CO_2 bubbles within the dissolution pipe, or the riser, of limited length (200–400 m). In this study, our previous model [Tsuchiya et al., 1997] is extended to bubbles containing lower-purity CO_2, which is more practical and realistic. For simplicity still, we consider the dissolution process of a single bubble (i.e., with negligible interaction with its neighboring ones) comprising two components of different solubility (in this case, A: CO_2 and B: N_2). The rate of transfer of each component can be represented based on the mass balance across the gas-liquid interface as

$$\frac{d(y_A n_b)}{dt}=\frac{d}{dt}\left(\frac{\pi}{6}d_e^3 y C_b\right)=-\pi d_e^2 N_A \tag{1}$$

$$\frac{d(y_B n_b)}{dt}=\frac{d}{dt}\left[\frac{\pi}{6}d_e^3 (1-y) C_b\right]=-\pi d_e^2 N_B \tag{2}$$

The effect of bubble-shape deformation on evaluating the true interfacial area for mass transfer is not accounted for due to the complexity involved in the shape fluctuations. Rearranging Eqs. (1) and (2) for the volume-equivalent bubble diameter, d_e, and the mole fraction of A, y ($\equiv y_A$), yields

$$\frac{dd_e}{dt}=-\frac{2}{C_b}\left(\frac{d_e}{6}\frac{dC_b}{dt}+N_A+N_B\right) \tag{3}$$

$$\frac{dy}{dt}=-\frac{6}{d_e C_b}[(1-y)N_A-yN_B] \tag{4}$$

The molar fluxes in the above equations are given by

$$N_A=k_{LA}(yC_{SA}-C_{LA}) \tag{5}$$

$$N_B=-k_{LB}(yC_{SB}) \tag{6}$$

The molar density of the gas within the bubble, C_b, is determined from the equation of state:

$$C_b=p_b/ZRT \tag{7}$$

where Z is the compressibility factor and p_b the pressure inside the bubble given as

$$p_b=p+4\sigma_L/d_e \tag{8}$$

by incorporating the effect of surface tension, σ_L, which is significant especially for small bubbles. Differentiating Eq. (7) with respect to time gives

$$\frac{dC_b}{dt}=-U_b C_b\left[\frac{\rho_L g}{p_b}-\left(1-\frac{p}{p_b}\right)\frac{d}{dz}(\ln d_e)-\frac{d}{dz}(\ln T)-\frac{d}{dz}(\ln Z)\right] \tag{9}$$

since the vertical coordinate of the bubble position in the GLAD riser is specified by

$$dz/dt=-U_b \tag{10}$$

While the surrounding liquid is of almost infinite extent for a single bubble rising in the riser, that in the present experiment is finite. The following mass balance then needs to be made:

$$\text{Rate} \equiv \pi d_e^2 k_{LA}(yC_{SA} - C_{LA}) = d(V_L C_{LA})/dt \quad (11)$$

which gives an estimate of the rate of increase in the background concentration of CO_2 in the bulk liquid of volume V_L:

$$dC_{LA}/dt = \text{Rate}/V_L \quad (12)$$

Eqs. (3), (4), (9), (10) and (12) are to be integrated simultaneously for obtaining the axial/vertical distributions of the bubble size and the CO_2 content within the gas phase, i.e., the rate of diminishing of a CO_2-containing bubble, with all the pertinent parameters being expressed in mathematical forms [Tsuchiya et al., 1997].

RESULTS AND DISCUSSION

Typical time variations in the bubble diameter are shown in Fig. 3 for two types of tap water with different contamination levels. The data are taken for the dissolution of CO_2 bubbles in circulating water pressurized at 0.2 MPa. d_e is evaluated at proper time intervals as soon as each injected bubble gets stabilized in free suspension (after on the order of several seconds). Note the plot is made so that at time t=0 s the bubble diameter is around 12 mm. As can be seen, especially in the lower figure, the initial bubble size (marked with filled symbols) has no appreciable effect on the bubble-diminishing rate over the initial rapid absorption period (t<10 s). Beyond this period, the diminishing rate becomes very slow and in 30 s, substantial part of the CO_2 dissolution process has reached near termination, leaving d_e finite and approaching asymptotic values. These asymptotic values correspond to the volume of gas which has been desorbed from the liquid to the bubble, i.e., N_2 used to pressurize the system.

Fig. 3 includes two lines which are obtained based on the present model specifically for the initial period [i.e., with $y \cong 1$ in Eq. (1)]. The broken line involves the liquid-phase mass transfer coefficient, k_L, expressed based on the boundary-layer modification of Higbie's surface renewal theory with a "surface-flow retardation" factor [Tsuchiya et al., 1997]; the solid line represents the model prediction with the liquid-phase agitation due to interactive bubbles [Calderbank and Moo-Young, 1961] taken into account. While the former line follows the data for "contaminated" tap water, the latter predicts the less contaminated case.

Fig. 4 shows the data obtained by Saito et al. [1999] using a larger-scale airlift column, along with those obtained in this study. The present results give slightly higher bubble-diminishing rate than the large-scale results during the initial period; the difference, however, becomes negligible after $t \cong 6$ s, as the data approach asymptotic values. The model prediction of both sets of data is improved by accounting for N_2 desorption. In contrast to the dot-dash line which represents the model prediction with only CO_2 absorption taken into account, the solid line representing the solution for the complete set of the differential equations given in the previous section can predict the entire dissolution process. The model calculation further characterizes the dissolution process by little change in the CO_2 mole fraction near unity followed by a transitory decrease down to zero, as depicted by the dotted line. This theoretical trend supports the experimental trend that a steady decrease in the bubble diameter occurs initially followed by no appreciable variation in

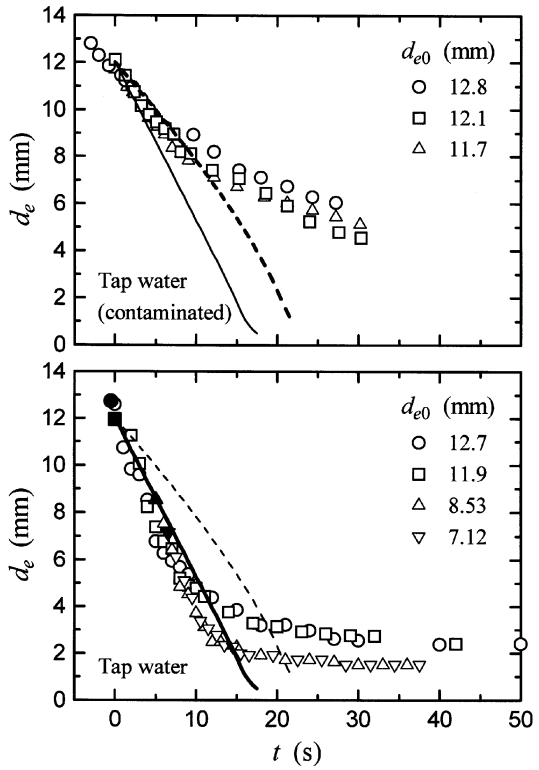

Fig. 3. Effect of liquid contamination level on bubble-diminishing rate.
– – – –: k_L estimated based on the modified Higbie's surface renewal theory [Tsuchiya et al., 1997]; ———: based on the correlation taking into account the liquid-phase turbulence [Calderbank and Moo-Young, 1961].

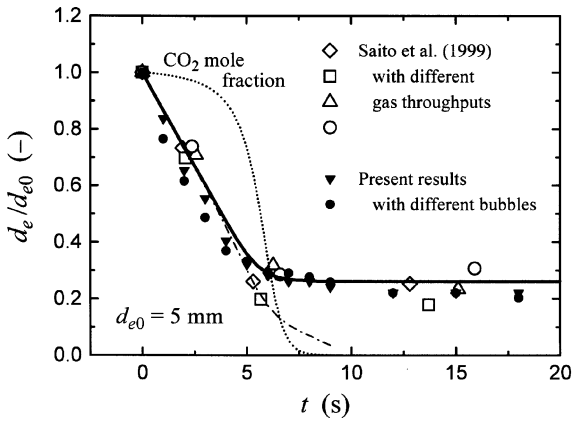

Fig. 4. Model performance evaluated based on two-different sets of experimental data.
–·–·–·–: bubble size with only CO_2 absorption taken into account; ———: bubble size with N_2 desorption taken into account as well; ·····: CO_2 mole fraction within the bubble.

the diameter. The transition is distinctive and its occurrence corresponds well between the experiment and the modeling.

Based on the above comparisons of the results, the present model can be simplified to

$$d_e = d_{e0} - 2(C_{SA}/C_b)k_{LA}t \quad (13)$$

which predicts the initial dissolution process as a constant-slope process in the d_e–t relationship. This implies that the mass transfer coefficient k_L can be estimated from the rate of reduction in the bubble diameter. Fig. 5 shows the average slopes evaluated over the initial dissolution period for all the liquids tested in this study. As seen in the figure, the slope or "apparent" mass transfer coefficient depends on the type of liquid used. The unerring difference in the k_L value exists between the two extreme cases, by a factor of four. This difference is substantiated by the distinctive difference in the extent of bubble-surface oscillations observed through visualization. Reflecting the "rigidity" of the gas-liquid interface affected by the liquid-phase contamination level or electrolyte concentration, the extent of the oscillations can be quantified statistically in terms of geometric parameters such as the bubble periphery-to-area ratio and the local curvature of surface ripples [Tsuchiya et al., 1997].

Fig. 6 shows the effects of the presence of satellite bubbles on the mass transfer rate from the primary bubble. The abscissa signifies the net duration of time when the primary and secondary bubbles contact, normalized with the total interactive time for a whole sequence of bubble-bubble interaction. The interaction with the satellite bubbles is found generally to suppress the dissolution of the primary bubble. The extent of reduction in the dissolution rate increases with the net contacting time. When the secondary bubbles interact with the primary bubble mainly outside of its wake, however, the dissolution tends to be enhanced due to induced turbulence in the surrounding liquid flow.

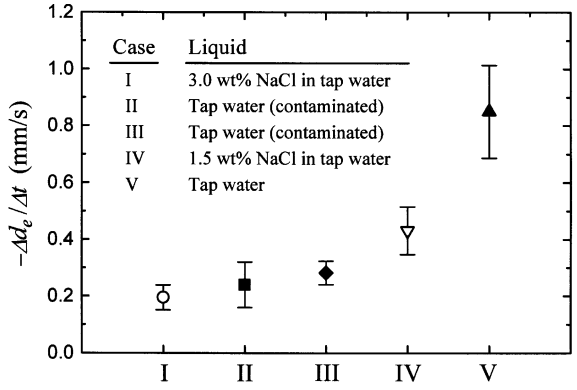

Fig. 5. Effect of liquid type on initial slope of bubble-diminishing rate.

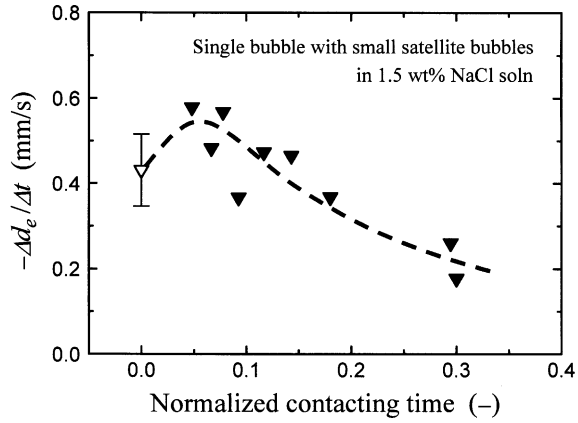

Fig. 6. Effect of bubble interaction on mass transfer rate.

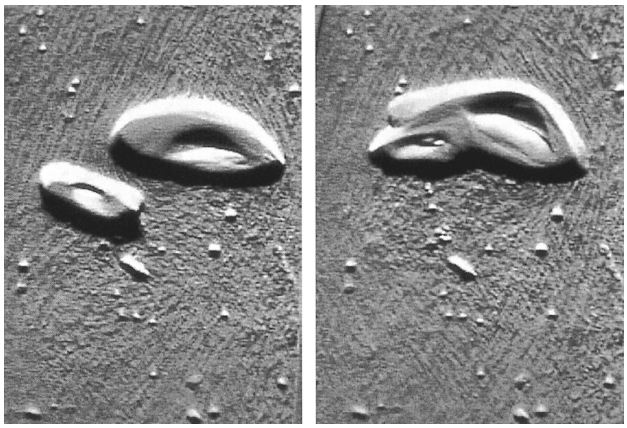

Fig. 7. Visualization of flow around interacting bubbles.

Fig. 7 shows two representative images of interacting bubbles taken by the high-sensitivity CCD camera and reproduced in the differential mode. The motion of tracer particles is clearly seen near the bubble surface. The image on the left corresponds to the case where the secondary bubble enhances the dissolution of the primary bubble by closely interacting with it but staying outside of its wake. The image on the right signifies the case where the secondary bubble contacts the primary bubble at the base. In this case, the effective area for mass transfer from the primary bubble is reduced, leading to the suppression of the dissolution rate.

CONCLUDING REMARKS

The physical model proposed in this study for single-bubble dissolution provides a useful evaluation basis for the GLAD performance on the CO_2 absorption. The effects of the rigidity of the gas-liquid interface and the presence of secondary bubbles on the dissolution rate of the primary bubble can be evaluated experimentally; in the model, however, these effects are difficult to account for with *a priori* estimation of parameters only. It is found that the simulation results are sensitive to the value of k_L estimated; for proper account of the present experimental findings, it is necessary to empirically correlate the k_L value. By "tuning" the model prediction to fit the initial part of the experimental data, the dependence of the mass transfer coefficient on the extent of bubble-surface oscillations and on the manner of bubble-bubble interactions could be incorporated into the model using, e.g., the integral boundary-layer approach.

ACKNOWLEDGMENT

The work was supported by the R&D Funds to Encourage

Competition among Research Institutes (Competitive Research Program) of the Agency of Industrial Science and Technology, MITI.

NOMENCLATURE

C_b : molar density of gas in the bubble [mol m^{-3}]
C_{LA} : concentration of CO_2 in the bulk liquid [mol m^{-3}]
C_{SA} : saturation concentration of CO_2 in the liquid at bubble surface [mol m^{-3}]
d_e : equivalent bubble diameter: diameter of a sphere having the same volume as the bubble [m]
g : gravitational acceleration [m s^{-2}]
N : molar flux [mol $m^{-2}s^{-1}$]
n_b : moles of gas in the bubble [mol]
k_L : liquid-phase mass transfer coefficient [m s^{-1}]
p : pressure in the liquid phase [Pa]
p_b : pressure in the bubble [Pa]
R : gas constant [J $mol^{-1}K^{-1}$]
T : temperature [K]
t : time [s]
U_b : bubble rise velocity relative to the liquid phase [m s^{-1}]
V_L : volume of the bulk liquid [m^3]
y : mole fraction of CO_2 in the bubble
Z : compressibility factor
z : vertical coordinate of the bubble position [m]

Greek Letters

ρ_L : liquid density [kg m^{-3}]
σ_L : surface tension [N m^{-1}]

REFERENCES

Calderbank, P. H. and Moo-Young, M. B., "The Continuous Phase Heat and Mass Transfer Properties of Dispersions," *Chem. Eng. Sci.*, **16**, 39 (1961).

Clift, R., Grace, J. R. and Weber, M. E., "Bubbles, Drops, and Particles," Academic Press, New York (1978).

Kawase, Y., Halard, B. and Moo-Young, M. B., "Liquid-Phase Mass Transfer Coefficients in Bioreactors," *Biotechnol. Bioeng.*, **39**, 1133 (1992).

Saito, T. and Kajishima, T., "Method and Apparatus for Dissolving and Isolating Carbon Dioxide Gas under the Sea," U.S. Patent **5662837** (1997).

Saito, T., Kajishima, T., Tsuchiya, K. and Kosugi, S., "Mass Transfer and Structure of Bubbly Flows in a System of CO_2 Disposal into the Ocean by Gas-Lift Column," *Chem. Eng. Sci.*, **54**, 4945 (1999).

Tsuchiya, K., Mikasa, H. and Saito, T., "Absorption Dynamics of CO_2 Bubbles in a Pressurized Liquid Flowing Downward and its Simulation in Seawater," *Chem. Eng. Sci.*, **52**, 4119 (1997).